ACS ORGANIC & INORGANIC Au
AN OPEN ACCESS JOURNAL OF THE AMERICAN CHEMICAL SOCIETY

pubs.acs.org/orginorgau
Perspective

When Pore Met Semi: Charting the Rise of Porous Metal Halide Semiconductors

Published as part of ACS Organic & Inorganic Au special issue "2025 Rising Stars in ACS Organic & Inorganic Au".

Ali Azmy, Alissa Brooke Anderson, Mina Bagherifard, Neelam Tariq, Kamal E. S. Nassar, and Ioannis Spanopoulos*

Cite This: ACS Org. Inorg. Au 2025, 5, 87−96
Read Online
ACCESS | Metrics & More | Article Recommendations

ABSTRACT: Metal halide semiconductors (MHS) are a versatile class of materials with fully customizable mechanical and optoelectronic properties that have proven to be prominent candidates in numerous impactful applications. Finding a way to generate porosity in MHS would bestow upon them an additional node in property engineering, thus allowing them to be utilized in uncharted technologies. Motivated by this promise, we developed a general strategy to render the MHS porous. We employed molecular cages as structure-directing agents and countercations, which fostered a new family of materials: porous metal halide semiconductors (PMHS). The presence of molecular cages gave rise to ultramicroporous structures imposed by the organic part cavities and a record water stability performance of 27 months so far. In this Perspective, we discuss the principles and promises of PMHS, which combine the merits of porous and electronic compounds.

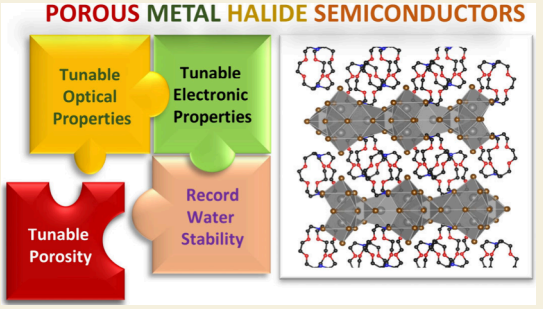

KEYWORDS: *semiconductors, metal halides, porosity, water stability, optical properties, molecular cages*

INTRODUCTION

Porous materials (PMs) can be uniquely equipped with properties that allow them to be utilized in various industrial applications, spanning from water purification and desalination[1] to heterogeneous catalysis,[2] gas storage,[3] and environmental remediation.[4] Their porous nature allows them to interact with atoms, ions, and molecules not only at their surfaces but also throughout the bulk of the material.[5,6] Although critical improvements in the material design of porous compounds were achieved over the last few decades, their advantageous traits were realized millennia ago. The adsorbent properties of native materials, such as clay, sand, and wood charcoal (synthesized unintentionally when making fire), were harnessed by the ancient Egyptians, Greeks, and Romans for the filtration of water, the clarification of fat and oil, and the treatment of indigestion (Figure 1).[5,7,8]

Activated charcoal was the first PM to reach the market.[20] It was incorporated in gas masks during World War I, while naturally occurring zeolite materials and their synthetic analogs were commercialized shortly after.[21,22] The need to remove lead from gasoline provided an economic incentive for the mass production of ZSM-5 (Zeolite Socony Mobil-5) zeolite, which was later employed for the MSTD (mobil selective toluene disproportionation) process. Currently, synthetic FAU (Faujasite-type) and MFI (Mobil Five) zeolites dominate several industrial applications, such as fluid catalytic cracking (FCC) processes in oil refining, converting methanol to gasoline (MTG), and *para*-xylene production.[23] The key to their success is a combination of attributes, such as water and thermal stability (up to 900 °C), tailorable acid−base character, nontoxic composition, and customizable porosity (pore size, pore dimensionality, and connectivity).[24]

Despite being quite competent PMs, due to their fully inorganic framework composition, zeolites offer limited structural flexibility in terms of acquired pore size distribution, total pore volume, and specific surface area (SSA). This deficiency in PM design was addressed by incorporating organic components in the structural composition, giving rise to hybrid (organic−inorganic) architectures.[25] Considering the plethora of reported hybrid PMs, we briefly mention the largest and most explored family of relevant compounds, known as

Received: December 10, 2024
Revised: January 6, 2025
Accepted: February 11, 2025
Published: February 28, 2025

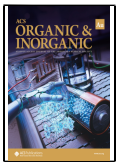

https://doi.org/10.1021/acsorginorgau.4c00093
ACS Org. Inorg. Au 2025, 5, 87−96

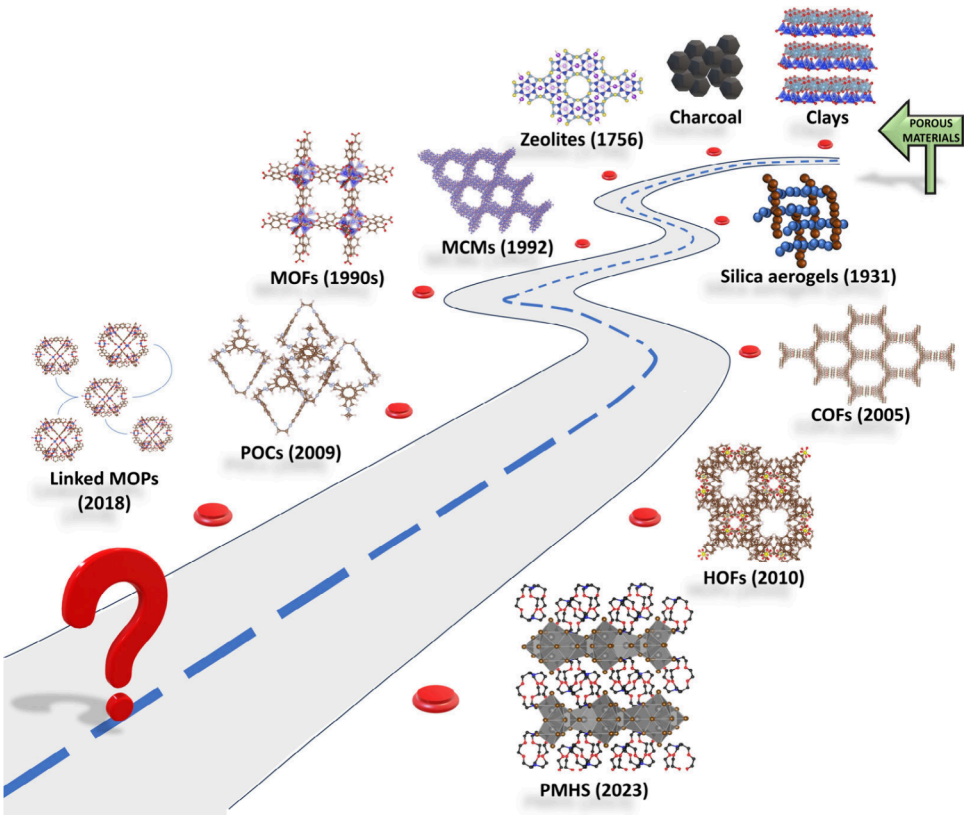

Figure 1. Evolution of PMs through the ages. The figure showcases a roadmap for PMs' structural evolution and diversity, starting with clay and charcoal,[9] silica aerogels,[10,11,12] zeolites, mobile composition of matter (MCM) mesoporous silica,[13] metal−organic frameworks (MOFs),[14] covalent−organic frameworks (COFs)[15] to porous organic cages (POCs),[16] linked metal−organic polyhedra (MOP), permanently porous hydrogen-bonded organic frameworks (HOFs),[1718] and the recently reported by us family of porous metal halide semiconductors (PMHS).[19]

metal−organic frameworks (MOFs) or porous coordination polymers (PCPs). Since the demonstration of tangible porosity in MOFs in the 1990s,[14,26] the field has advanced significantly by addressing long-term structural stability concerns and demonstrating their potential in unexpected applications, such as water harvesting[27,28] and triboelectric nanogenerators (TENGs). The fully customizable pore dimensions and framework composition constitute the corresponding fourth generation MOFs capable of capturing and releasing H_2O reversibly and promoting charge generation and transfer for energy harvesting.[29]

Porosity generation is considered an important trait for tuning material properties; hence, it has sparked interest across fields. In 1955, Uhlir and his wife Ingeborg (who performed the experiments) applied electrolytic etching to Si and Ge as a means of smooth mechanical shaping of metals and semiconductors.[30] Not until three decades later did scientists realize that the same technique could create controlled porosity in inorganic semiconductors. This set the foundation for a new family of multifunctional materials, making them suitable for uncharted applications, such as photocatalysis, energy storage, integrated waveguides, and photonic crystals.[31−33]

Porous Si-based structures featured photoluminescence across the range from the near-infrared (∼1.5 mm) through the visible region and into the near UV. This is truly remarkable, considering that bulk Si is inefficient at emitting light, even at cryogenic temperatures.[34,35] The presence of cavities in mesoporous Ge reduced its thermal conductivity substantially, which was found to be 2 orders of magnitude lower (0.6 W/(m K)) than that of bulk Ge substrates (58 W/(m K)).[36,37] Anodic etching of n-type GaP induced porosity, which increased the quantum yield for light-to-current conversion from extremely low values to unity for light absorbed in the indirect optical transition.[38] Porous InP(100) was reported to feature a significantly enhanced radiated terahertz field (20 times) and second-harmonic radiation (30 times) emission relative to the bulk, nonporous InP(100) material.[39] Introducing 30 nm pores into GaN can substantially tune its refractive index and birefringence, showcasing a decrease in the refractive index when the porosity is increased.[40] Photoelectrochemical etching of CdSe improved the output characteristics of a CdSe−polysulfide photoelectrochemical cell by increasing both the short-circuit current and fill factor.[41]

METAL HALIDE SEMICONDUCTORS

Hybrid metal halide semiconductors (MHS), including halide perovskites, are a family of materials with fine-tunable optical,[42] electrical,[43] electronic,[44] and mechanical properties[45] that hold great promise for terrestrial and space applications.[46] It is pointed out that due to their hybrid nature it is possible by means of molecular and crystal engineering to design compounds with a combination of properties that cannot be found in any other fully organic or fully inorganic semiconductor. These attributes include their low-cost solution processability,[47] long carrier lifetimes,[48] diffusion lengths,[49,50] high radiation damage tolerance,[51−53] high light absorption coefficients, and self-healing capabilities.[54,55]

https://doi.org/10.1021/acsorginorgau.4c00093
ACS Org. Inorg. Au 2025, 5, 87−96

Considering these characteristics, it is safe to hypothesize that rendering MHS porous could introduce an additional fine-tunable node in their properties' arsenal, unlocking new applications or enhancing the efficiency of those already established. In particular, the presence of cavities could enhance their catalytic performance by increasing the SSA, while size-selective pore architecture can promote substrate/product selectivity.[56−58] Considering their significantly lower synthesis and composition cost, MHS poses a promising alternative to current state-of-the-art catalysts based on expensive platinum group metals (PGMs).

On a different aspect, halide perovskites feature both electronic and ionic conductivity, the latter originating from halide ion migration enabled by point defects.[59,60] Therefore, corresponding materials could be deployed to assemble mixed ion/electron-conducting (MIEC) scaffolds or interlayers for next-generation solid-state batteries (SSBs).[61,62] This stems from the fact that cavities with tunable dimensions can allow the incorporation of specific alkali metal ions (e.g., Li^+, Na^+, and K^+) in the structure. In return, porous MHS loaded with alkali metal cations would offer advantages in SSB design, such as reduced local current density, uniform and better ion flux promotion, dendrite growth suppression, reduced mechanical stress (during charge and discharge), and improved charge density.

STRATEGIES TO GENERATE POROSITY

The next step in material design is identifying a proper synthetic method to generate porosity in MHS. Some of the most common strategies to acquire porous, fully inorganic materials involve the templating method or the electrochemical dissolution (etching) method.[63,64] Two types of templating approaches can be distinguished, i.e., the soft templating process in which the templates are usually amphiphilic molecules like surfactants or block copolymers and the hard templating approach using preformed mesoporous silica/carbon as the template matrix.[65,66] By removing the template, a porous structure can be formed. In the case of pore formation through dissolution, three methods can be distinguished: chemical, electroless, and anodic dissolution. Part of the material is dissolved in each of these types of materials to generate cavities. Regarding porous fully inorganic semiconductors, targeted partial structure dissolution served as a facile tool to customize pore architectures irrespective of material composition. However, in the case of MHS, the dissolution method cannot be employed, as it will lead to structural degradation. Similarly, the use of templates may give rise to elaborate functional motifs, but if the templates are part of the structure (serving, e.g., as counterions), then they cannot be removed without structural collapse. This is the case in the family of so-called "open-framework metal halide materials"[67] where the use of organic cations as structure-directing agents such as tetrakis(*N*-imidazolemethylene)-methane (TIMM),[68] 2,2-bipyridine,[69,70] DABCO (1,4-diaza-bicyclo[2.2.2]-octane),[71] TPT (*N*-methylated 2,4,6-tri(4-pyr-idyl)-1,3,5-triazine,[72] and DMBTz (dimethylbenzotriazo-lium)[70] gives rise to 3D framework architectures with cavities and channels. However, these organic molecules occupy the formed pores as countercations. They are part of the structure and cannot be removed without affecting the material's structural integrity, ergo rendering them nonporous. The lack of porosity, here termed the accessible internal surface area, is further supported by the absence of gas sorption studies to validate the porous nature. If the pores are filled with organic compounds, then they are inaccessible by molecules in the gas or liquid phase, thus hindering the implementation of these materials in applications where porosity is essential. Recently, a strategy for creating porous 2D halide perovskites has been proposed. Kataoka et al. used polyhedral oligomeric silsesquioxane (POSS) as a templating agent among the 2D perovskite layers of various metal halides.[73,74] Although gas sorption studies using N_2 at 77 K are reported, there is limited structural evidence to confirm that the measured gas uptake correlates to a porous 2D perovskite structure. The reported single crystal structure is not a proper perovskite (lack of corner-sharing MX_6 octahedra). At the same time, there is no association between the experimental and calculated total pore volumes and pore size distribution. These studies are essential to validate that the sorption data are directly derived from the porous crystal structure. We point out that consistency criteria must also be applied to demonstrate the robustness of the sorption studies.[75,76]

It is essential to acknowledge that various fully organic and hybrid porous semiconductor materials have been reported before.[77] Li et al. synthesized an organic semiconductor, 2,6-di(2-naphthyl)anthracene (dNaAnt), where single-crystal field-effect transistors show mobility up to 12.3 $cm^2 \cdot V^{-1} \cdot s^{-1}$ and a photoluminescence quantum yield (PLQY) of 29.2%.[78] Liu et al. reported a semiconducting metal−organic framework (MOF), namely, Cu_2 (TCPP) (TCPP = meso-tetra(4-carboxyphenyl)porphine),[79] with a band gap of 2.19 eV adopted for the assembly of field-effect transistors (FETs). Byun et al. assembled semiconducting porous organic polymers (POPs), e.g., p-POP,[80] with a band gap of 0.65 eV and a conductivity of 5×10^{-8} S cm^{-1}, while Bi et al. synthesized semiconducting covalent organic frameworks (COFs), where one member, g-$C_{40}N_3$−COF featured an optical band gap of 2.36 eV, coupled by a 0.7% PLQY.[81] Despite their promising semiconducting performance, they lack multiple features of hybrid perovskite and metal halide materials, such as superior light absorption, solution processability, mixed ionic−electronic conductivity, and fine-tunable optical properties.

POROUS METAL HALIDE SEMICONDUCTORS (PMHS)

Inspired by MHS's plethora of beneficent properties and the immense potential of creating a new family of materials upon porosity generation, we undertook the synthetic challenge.

The Challenge

The hybrid nature bestows upon the corresponding materials unique versatility in material design. This stems from the fact that by employing molecular engineering custom-made organic molecules of various geometries and sizes can serve as counterions and/or structure-directing agents based on the type of functional groups they bear. In the case of hybrid MHS, the organic part of the material cannot be removed from the structure, for example, by heating, as in the case of porous, fully inorganic semiconductors,[82] because the organic linker acts as a countercation charge balancing the structure.[83] Therefore, any attempt to remove it will lead to structural collapse. This structural feature hinders the use of elaborate activation protocols (such as supercritical CO_2) currently implemented in other PMs such as MOFs (Figure 2). Similarly, one could

https://doi.org/10.1021/acsorginorgau.4c00093
ACS Org. Inorg. Au 2025, 5, 87−96

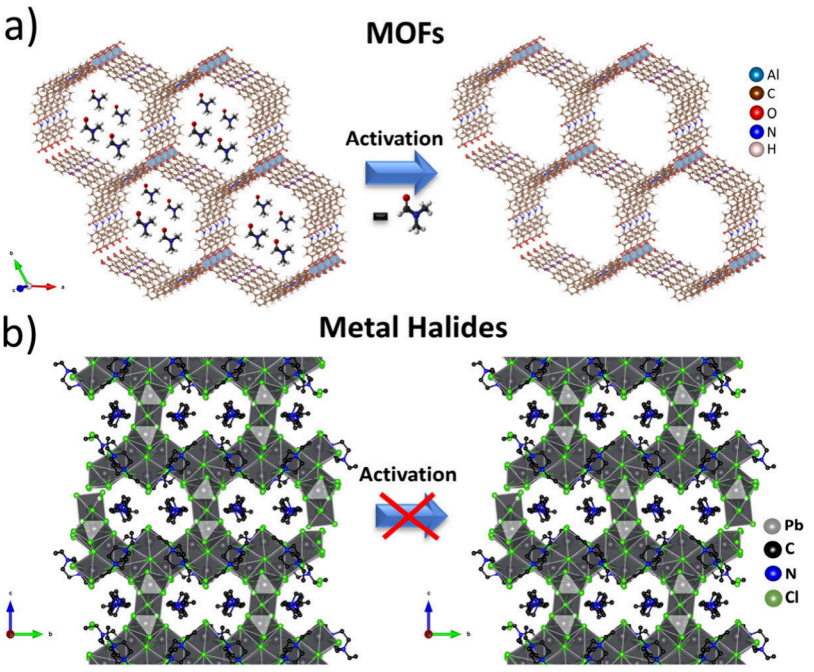

Figure 2. a) Various activation protocols can remove the solvent molecules from MOF cavities, giving rise to accessible internal surface area. b) Removal of countercations from open framework metal halides[71] is not possible as it will lead to structural collapse.

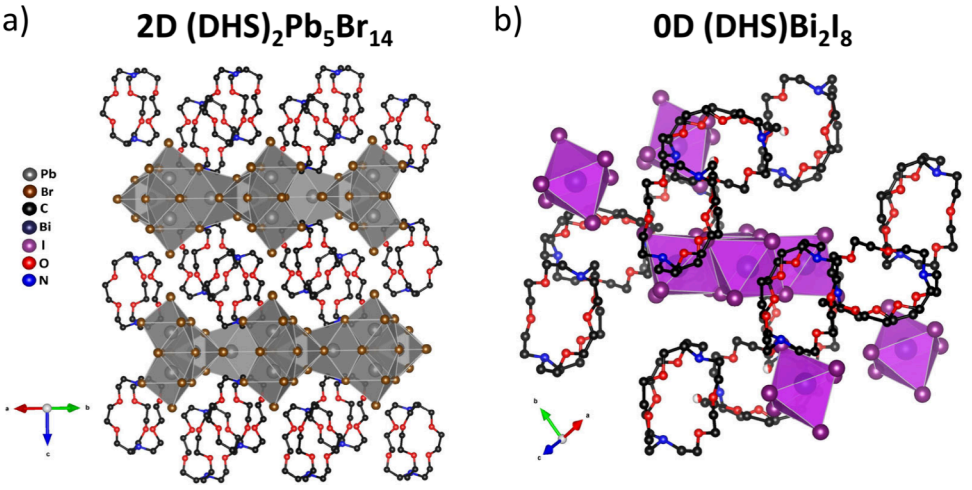

Figure 3. Part of the crystal structures of a) $(DHS)_2Pb_5Br_{14}$ across the [110] direction (in-plane) and b) $(DHS)Bi_2I_8$. Hydrogen atoms and disordered lead, bromide, and carbon atoms are omitted for clarity.

propose the exchange of the bulkier organic ligands with much smaller cations (e.g., NH_4^+, $CH_3NH_3^+$) that could ensure that the charge balance of the framework is preserved. A corresponding size mismatch between the former and latter countercations is expected to create accessible space in the pore network, as it is regularly showcased in ionic MOFs.[84] However, in the absence of a proper pore network in MHS that would allow the complete replacement of bulky countercations with smaller ones, this strategy might prove impossible for generating accessible surface area. Furthermore, even if complete ligand replacement is feasible, it is unclear whether the cation-exchanged material could maintain its structural integrity. That remains to be tested.

The Solution

Considering the above, we took a different approach to tackle the problem. For hybrid materials, the presence of the organic part is essential for the structural integrity. Therefore, is it possible to acquire a porous material by taking advantage of the nature of the organic ligand? This can be achieved by adopting a suitable porous organic molecule acting as both a structure-directing agent and a countercation. At the same time, the presence of pores in the ligand could give rise to a hybrid PM. Of course, in this case, for the material to be considered porous, the whole pore network must be fully accessible by the incoming gas or liquid probe molecules.

To test our hypothesis, we utilized molecular cages targeting the synthesis of hybrid MHS materials. We started with the [2.2.2] cryptand (DHS) molecule, which bears two tertiary amine groups that can be protonated, thus serving as countercations for the anionic inorganic framework. Indeed, the reaction of DHS with Pb^{2+} in HBr gave colorless hexagonal crystals. Single crystal X-ray diffraction (XRD) studies revealed a unique structural motif of a 2D metal halide material with

https://doi.org/10.1021/acsorginorgau.4c00093
ACS Org. Inorg. Au 2025, 5, 87−96

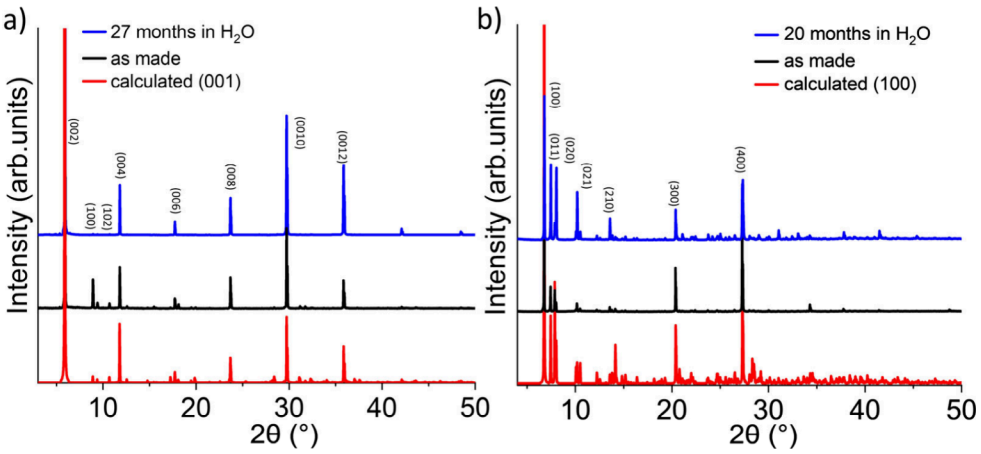

Figure 4. Comparison of PXRD patterns for the as-made materials and the water-treated ones, to the calculated patterns derived from the solved single crystal structures (including preferred orientation) for a) $(DHS)_2Pb_5Br_{14}$ and b) $(DHS)Bi_2I_8$. We note that these materials are porous, and the presence of molecules within their cavities (e.g., H_2O from incomplete drying) can influence the electron density distribution among planes (e.g., (100)). This, in turn, affects the relative diffraction intensities observed in corresponding PXRD studies, where differences can arise when calculated diffraction patterns (assuming no H_2O molecules) are compared with experimental results, where H_2O molecules may fully or partially occupy the cavities.

formula $(DHS)_2Pb_5Br_{14}$ (Figure 3a) that crystallizes in the hexagonal space group $P6_3/m$.[19] The inorganic layer is formed by face-sharing $[Pb_5Br_{23}]^{13-}$ clusters, each one consisting of two face-sharing $PbBr_7$-capped trigonal prisms that share faces with three $PbBr_8$ hendecahedra. This cluster connectivity gives rise to a hexagonal cavity of 7.6 Å in diameter within the inorganic layer, while adjacent inorganic layers are staggered, lying at a distance of 4.0 Å. We point out that this is not a Lindqvist-type cluster (typically composed of MO_6 (M = V, Mo, W, Nb, Ta) octahedra with the formula $[M_6O_{19}]^{2-/8-}$, where six M atoms are joined together through a μ_6-O bridging atom to generate a $[\mu_6\text{-}OM_6]$ octahedron),[85,86] and to the best of our knowledge, is unprecedented for lead halide materials.[67] The 2D inorganic layers are separated and charge-balanced by a single layer of DHS organic countercations, which are staggered along the *a* axis at a distance of 2.1 Å, exhibiting a brick-work-type arrangement. Along the *c* axis, a hexagonal arrangement motif is revealed, templated by the protruding $PbBr_7$-capped trigonal prisms at the center of the hexagonal cavity.

The second member of this family of materials is the lead-free analog $(DHS)Bi_2I_8$, which was synthesized by the reaction of Bi(III) oxide and the DHS linker in a hot HI solution.[87] Single crystal X-ray diffraction (XRD) studies revealed a 0D structure that crystallizes in the monoclinic space group $P2_1/c$ (Figure 3b). It consists of tetramers of edge-sharing $[BiI_6]^{3-}$ octahedra that are separated and charge-balanced by the DHS ligands. The overall connectivity of the centrosymmetric tetranuclear anion can be described as a pair of edge-sharing bioctahedra, which mutually share two and three cis edges, respectively. The organic countercations are eclipsed along the *a* axis, laying at a distance of 2.7 Å, revealing a hexagonal arrangement motif, templated by the protruding axial iodide atoms of the tetramer.

The acquisition of two different materials using the same organic ligand shows that DHS can serve as a countercation, templating higher- and lower-dimensional structures. The question arises whether the corresponding materials are actually porous and whether gas probe molecules have access to the whole pore network. Corresponding compounds constitute a new family of materials, namely, porous metal halide semiconductors (PMHS). In the next sections, the properties of these compounds are compared and discussed in detail.

PMHS PROPERTIES

Water Stability

A very surprising outcome of this strategy was the fact that both aforementioned compounds have been water-stable for 20 and 27 months so far, a record stability performance among hybrid halide semiconductors, including MOFs.[88] A comparison of the PXRD patterns from the fresh and water-aged powder samples (Figure 4) reveals that the materials retain their highly crystalline nature and phase purity after water immersion. Calculated full width at half-maximum (fwhm) values for the strongest diffraction peaks ((002) for $(DHS)_2Pb_5Br_{14}$ and (100) for $(DHS)Bi_2I_8$) are 0.04 before and after the water treatment for both analogs. Meanwhile, there is no appearance of additional diffraction peaks, indicative of structure degradation. Considering the compositional differences and structure dimensionality, 2D versus 0D for $(DHS)_2Pb_5Br_{14}$ and $(DHS)Bi_2I_8$, respectively, we believe that water stability derives from the organic part of the structure and not from structure dimensionality. According to current studies, only one H_2O molecule can fit into the DHS cage (supported by DFT and sorption analysis); therefore, we hypothesize that once the pores are filled with H_2O additional incoming water molecules do not have access to the inorganic part of the structure. The filled pores form a type of barrier, thus protecting the inorganic part of the structure from degradation. Nonetheless, further studies and new PMHS materials are required to elucidate this performance.

Porosity

The critical question that arises is whether the corresponding materials are actually porous. This can be demonstrated in a solid manner by performing gas and vapor sorption studies. Interestingly, N_2 sorption studies at 77 K and CO_2 studies at 195 K revealed no gas uptake. Performing a sorption measurement at the boiling point of the probe molecules is

https://doi.org/10.1021/acsorginorgau.4c00093
ACS Org. Inorg. Au 2025, 5, 87−96

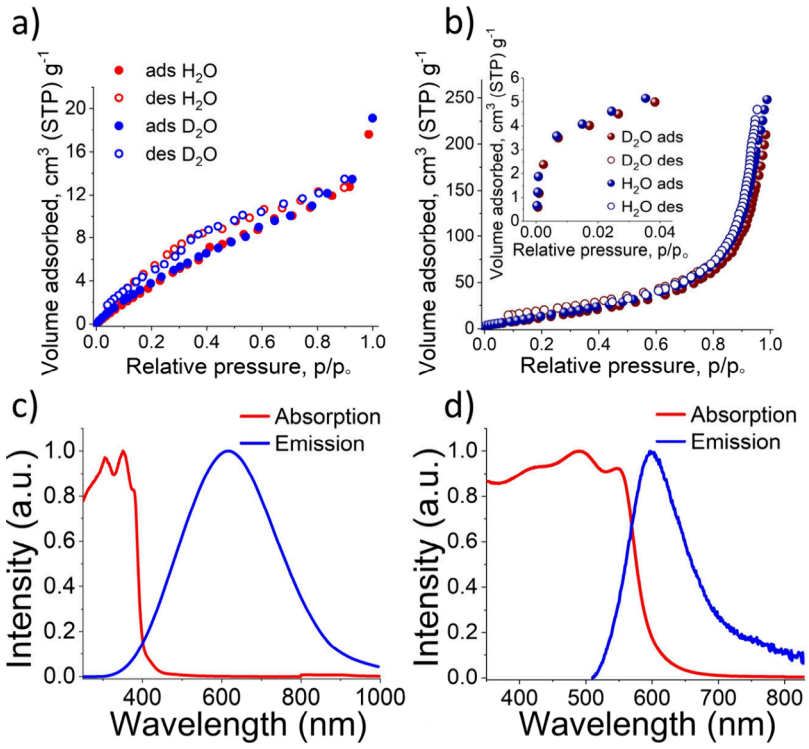

Figure 5. Vapor-sorption isotherms for H_2O and D_2O at 298 K for a) $(DHS)_2Pb_5Br_{14}$ and b) $(DHS)Bi_2I_8$. The recorded absorption and emission spectra of c) $(DHS)_2Pb_5Br_{14}$ and d) $(DHS)Bi_2I_8$ at RT. Reproduced with permission from ref 87. Copyright 2023, American Chemical Society. Adapted with permission from ref 19. Copyright 2023, Wiley-VCH GmbH.

essential to determine total pore volume, pore size distribution, and SSA determination. Benefitted by the water stability of PMHS materials, we performed H_2O and D_2O sorption studies at RT. Notably, the compounds revealed a fully reversible and a closed-loop sorption isotherm indicative of the physisorption of H_2O and D_2O molecules into the framework (Figure 5a,b). We point out that H_2O has a much smaller kinetic diameter (2.65 Å) than N_2 (3.64 Å) and CO_2 (3.30 Å).[89] Therefore, corresponding materials are considered to be ultramicroporous (≤3 Å pore size), serving as molecular sieves, permeable only by water molecules.[90,91] It was recorded that the total vapor uptake in both cases corresponded to one water molecule per cage cavity, which was fully consistent with density functional theory (DFT) studies, revealing that only one water molecule can fit into the cage. Moreover, 2D $^1H-^1H$ exchange spectroscopy solid-state NMR studies confirmed the proximity of H_2O protons to the DHS linker's $-NH$ and $-CH_2-$ protons, validating that H_2O molecules reside in the formed cage cavities and not just on the surface of the crystallites.

It is pointed out that if the materials were not water-stable then vapor sorption studies (H_2O, D_2O) could not have been performed. Since there was no N_2 and CO_2 uptake, we could not call PMHS porous, thus hindering the discovery of this new family of compounds.

Semiconducting Nature

In addition to the water stability and porosity, the materials maintained their semiconducting nature. Based on DFT studies, both compounds are direct band gap semiconductors. Of course, due to their distinct composition, corresponding optical properties varied significantly.

Examining first the 2D $(DHS)_2Pb_5Br_{14}$, broad light emission at RT was recorded centered at 617 nm with a very large fwhm of 284 nm (0.96 eV) coupled by an average PL decay lifetime of 3.5 ns, typical for broad light emitting materials with similar composition (Figure 5c). Variable power PL studies elucidated that PL intensity saturates at high power flux, suggesting that the emission stems from the presence of permanent defects. On the other hand, $(DHS)Bi_2I_8$ features broad, band-edge light emission centered at 600 nm (2.06 eV) with a full width at half-maximum (fwhm) of 99 nm (0.33 eV), which is accompanied by an average PL decay lifetime of 3 ns (Figure 5d). Notably, after several months in water, the PLE and UV–vis spectra of the water-treated crystals match those derived from the fresh crystals, demonstrating the robustness of the optical properties.

Antibacterial Activity

Motivated by recent studies demonstrating the antibacterial performance of Bi(III) halides,[92,93] we tested $(DHS)Bi_2I_8$ against *Escherichia coli* (*E. coli*), methicillin-resistant *Staphylococcus aureus* MRSA, methicillin-resistant *Staphylococcus epidermidis* (MRSE), vancomycin-resistant *Enterococcus faecium* (VREF), *K. pneumonia*, and *P. aeruginosa*. Evidently, $(DHS)Bi_2I_8$ features broad-spectrum bactericidal activity against most targeted bacteria. Fluorescence microscopy and TEM studies shed light on the underlying mechanism, revealing that the bacteria cell membrane ruptures in the presence of $(DHS)Bi_2I_8$. We hypothesize that the generation of reactive oxygen species (ROS) is responsible for this performance, similar to the antibacterial behavior of TiO_2 and SnO_2 semiconductors.[94,95]

Considering the combination of multiple diverse properties, into a single material (record water stability, tunable optical and electronic properties, and tunable porosity), PMHS provide encouraging prospects for a plethora of applications.

https://doi.org/10.1021/acsorginorgau.4c00093
ACS Org. Inorg. Au 2025, 5, 87–96

PMHS PROMISES

Based on the reported PMHS compounds, generating porosity in MHS is now possible. In addition, our strategy solved a major deficiency of MHS compounds, moisture/water instability, probably in a permanent manner. Considering the structural versatility of hybrid materials, we are currently working on expanding the family of PMHS, targeting both fine-tunable porosity and optoelectronic properties. It would also be interesting to identify whether the presence of cavities can slow down Sn^{2+} or Ge^{2+} oxidation, thus allowing corresponding compounds to be employed toward the replacement of toxic Pb^{2+} for optoelectronic applications.

PMHS can also be used as capping layers in solid-state solar cell devices, improving device operational stability, as was recently demonstrated by the incorporation of molecular cages to improve device stability in air.[96] The challenge in this application is whether PMHS can hinder carrier transport. Based on the organic part composition and polar functional groups' presence, the cages' dielectric properties can be adjusted to hinder or promote dielectric confinement, thus facilitating carrier transport. Furthermore, the combination of water stability, porosity, semiconduction, and tunable optoelectronic properties paves the way for evaluating PMHS for energy- and environment-related applications (Figure 6). They

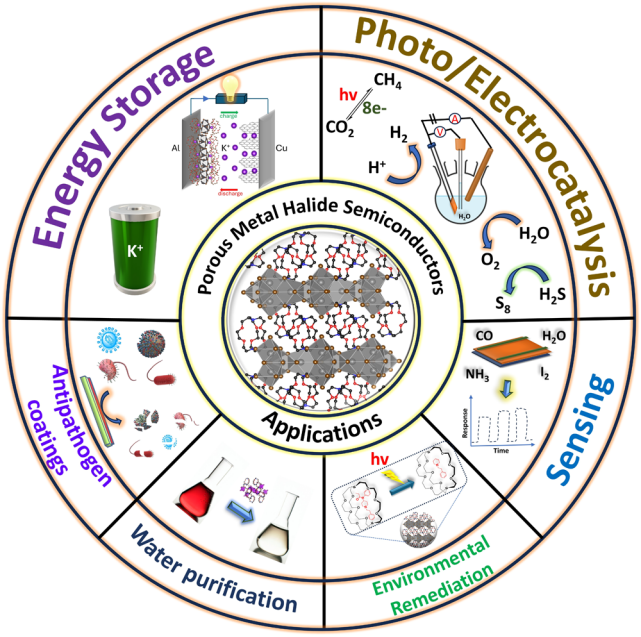

Figure 6. Potential applications of PMHS span energy storage and environmental remediation, to antipathogen coatings and water purification.

pose as promising catalysts for the generation of clean fuels and valuable commodities via photo- or electrocatalysis (hydrogen evolution reaction (HER), oxygen evolution reaction (OER), CO_2 reduction, N_2 fixation, H_2S oxidation) and the assembly of next-generation SSBs (see the "Metal Halide Semiconductors" section above). Moreover, due to the fact that these compounds are permeable only by water molecules and exhibit antipathogen performance, they can be leveraged for water desalination, water purification, and disinfection applications. Furthermore, designing PMHS that can be activated using visible light, e.g., $(DHS)Bi_2I_8$, can offer potentially continuous antibacterial performance, rendering them ideal for antibacterial coatings on everyday touched surfaces (e.g., door handles), personal protective equipment (e.g., gloves, masks), and medical devices (e.g., catheters, respirators). The challenge is whether corresponding films/coatings exhibit the same antipathogen performance and water stability as the bulk, single crystalline materials. Meanwhile, it would be interesting to identify if biocompatible, Bi(III)-based PMHS can be effective against other pathogens and select agents, solidifying their candidacy for applications relevant to national security.

Molecular engineering is expected to play a major role in the design of PMHS compounds with tunable porosity, while a question that arises is whether probe molecules could have access to the whole porous network regardless of structure dimensionality and pore architecture. A critical target in materials design is permanent water stability, a big deficiency of MHS. It would be interesting to render this issue obsolete, irrespective of the structure composition. These features present significant synthetic challenges. However, we remain confident that the combined power of scientific intuition, creative thinking, and interdisciplinary collaboration will overcome these hurdles.

CONCLUSIONS

By means of molecular and crystal engineering, porosity generation is now feasible in MHS, giving rise to a new family of materials, PMHS. Compared to other proposed methods, our ubiquitous strategy can give rise to porous and water-stable MHS irrespective of structure dimensionality (2D, 1D, and 0D). This Perspective discusses the emergence of PMHS, their synthesis, properties, and potential applications. This new node in material properties is expected to be fine-tunable, giving rise to an MHS with tailor-made cavities through molecular engineering. One very important characteristic is that the presence of pores had no impact on their semiconducting nature, which is of paramount importance for optoelectronic applications. Notably, all reported PMHS are direct band gap semiconductors. An impressive feature of our strategy is that corresponding materials have been water-stable for 27 months so far, a record stability performance for MHS compounds. While it is too early to claim that environmental instability has been entirely overcome, this achievement represents a significant step toward MHS commercialization. This unique combination of properties amassed by PMHS compounds paves the way for their utilization in numerous impactful applications spanning energy storage and clean fuel generation to environmental remediation and water disinfection. We believe the multifaceted nature of PMHS will attract interest across fields, as understanding how porosity influences optoelectronic and ionic properties, environmental stability, and antipathogen activity may lead to new material discoveries and uncover unexpected properties.

ASSOCIATED CONTENT

Data Availability Statement

The data underlying this study are available in the published article.

https://doi.org/10.1021/acsorginorgau.4c00093
ACS Org. Inorg. Au 2025, 5, 87−96

AUTHOR INFORMATION

Corresponding Author

Ioannis Spanopoulos − *Department of Chemistry, University of South Florida, Tampa, Florida 33620, United States;* orcid.org/0000-0003-0861-1407; Email: spanopoulos@usf.edu

Authors

Ali Azmy − *Department of Chemistry, University of South Florida, Tampa, Florida 33620, United States*

Alissa Brooke Anderson − *Department of Chemistry, University of South Florida, Tampa, Florida 33620, United States*

Mina Bagherifard − *Department of Chemistry, University of South Florida, Tampa, Florida 33620, United States*

Neelam Tariq − *Department of Chemistry, University of South Florida, Tampa, Florida 33620, United States*

Kamal E. S. Nassar − *Department of Chemistry, University of South Florida, Tampa, Florida 33620, United States*

Complete contact information is available at: https://pubs.acs.org/10.1021/acsorginorgau.4c00093

Notes

The authors declare no competing financial interest.

ACKNOWLEDGMENTS

This Perspective is based upon work supported by the U.S. Department of Energy, Office of Science, Office of Basic Energy Sciences, under Award Number DE-SC0025485.

REFERENCES

(1) Dutta, S.; de Luis, R. F.; Goscianska, J.; Demessence, A.; Ettlinger, R.; Wuttke, S. Metal-Organic Frameworks for Water Desalination. *Adv. Funct. Mater.* **2024**, *34*, 2304790.

(2) Chai, Y.; Dai, W.; Wu, G.; Guan, N.; Li, L. Confinement in a Zeolite and Zeolite Catalysis. *Acc. Chem. Res.* **2021**, *54*, 2894−2904.

(3) Spanopoulos, I.; Tsangarakis, C.; Klontzas, E.; Tylianakis, E.; Froudakis, G.; Adil, K.; Belmabkhout, Y.; Eddaoudi, M.; Trikalitis, P. N. Reticular Synthesis of HKUST-like tbo-MOFs with Enhanced CH_4 Storage. *J. Am. Chem. Soc.* **2016**, *138*, 1568−1574.

(4) Ge, S.; Wei, K.; Peng, W.; Huang, R.; Akinlabi, E.; Xia, H.; Shahzad, M. W.; Zhang, X.; Xu, B. B.; Jiang, J. A comprehensive review of covalent organic frameworks (COFs) and their derivatives in environmental pollution control. *Chem. Soc. Rev.* **2024**, *53*, 11259−11302.

(5) Robens, E. Some intriguing items in the history of adsorption. In *Stud. Surf. Sci. Catal.*; Rouquerol, J., Rodríguez-Reinoso, F., Sing, K. S. W., Unger, K. K., Eds.; Elsevier, 1994; Vol. *87*, pp 109−118.

(6) Rodríguez-Reinoso, F.; Rouquerol, J.; Unger, K. K.; Sing, K. *Characterization of Porous Solids III*; Elsevier Science & Technology: San Diego, Netherlands, 1994.

(7) Bryan, C. P.; Smith, G. E. *Ancient Egyptian medicine: the Papyrus Ebers*; Ares Publishers: Chicago, 1930.

(8) Aristotle; Lee, H. D. P. *Meteorologica*; Harvard University Press, William Heinemann: Cambridge, Mass., London, 1952.

(9) Brindley, G. W.; Robinson, K. The structure of kaolinite. *Mineralogical Magazine and Journal of the Mineralogical Society* **1946**, *27*, 242−253.

(10) Kistler, S. S. Coherent Expanded Aerogels and Jellies. *Nature* **1931**, *127*, 741−741.

(11) Barrer, R. M.; Rideal, E. K. The sorption of polar and non-polar gases by zeolites. *Proc. R. Soc. London, Ser. A* **1938**, *167*, 392−420.

(12) Cronstedt, A. Natural zeolite and minerals. *Svenska Vetenskaps Akademiens Handlingar Stockholm* **1756**, *17*, 120.

(13) Kresge, C. T.; Leonowicz, M. E.; Roth, W. J.; Vartuli, J. C.; Beck, J. S. Ordered mesoporous molecular sieves synthesized by a liquid-crystal template mechanism. *Nature* **1992**, *359*, 710−712.

(14) Li, H.; Eddaoudi, M.; O'Keeffe, M.; Yaghi, O. M. Design and synthesis of an exceptionally stable and highly porous metal-organic framework. *Nature* **1999**, *402*, 276−279.

(15) Côté, A. P.; Benin, A. I.; Ockwig, N. W.; O'Keeffe, M.; Matzger, A. J.; Yaghi, O. M. Porous, Crystalline, Covalent Organic Frameworks. *Science* **2005**, *310*, 1166−1170.

(16) Tozawa, T.; Jones, J. T. A.; Swamy, S. I.; Jiang, S.; Adams, D. J.; Shakespeare, S.; Clowes, R.; Bradshaw, D.; Hasell, T.; Chong, S. Y.; Tang, C.; Thompson, S.; Parker, J.; Trewin, A.; Bacsa, J.; Slawin, A. M. Z.; Steiner, A.; Cooper, A. I. Porous organic cages. *Nat. Mater.* **2009**, *8*, 973−978.

(17) Carné-Sánchez, A.; Craig, G. A.; Larpent, P.; Hirose, T.; Higuchi, M.; Kitagawa, S.; Matsuda, K.; Urayama, K.; Furukawa, S. Self-assembly of metal-organic polyhedra into supramolecular polymers with intrinsic microporosity. *Nat. Commun.* **2018**, *9*, 2506.

(18) Yang, W.; Greenaway, A.; Lin, X.; Matsuda, R.; Blake, A. J.; Wilson, C.; Lewis, W.; Hubberstey, P.; Kitagawa, S.; Champness, N. R.; Schröder, M. Exceptional Thermal Stability in a Supramolecular Organic Framework: Porosity and Gas Storage. *J. Am. Chem. Soc.* **2010**, *132*, 14457−14469.

(19) Azmy, A.; Li, S.; Angeli, G. K.; Welton, C.; Raval, P.; Li, M.; Zibouche, N.; Wojtas, L.; Reddy, G. N. M.; Guo, P.; Trikalitis, P. N.; Spanopoulos, I. Porous and Water Stable 2D Hybrid Metal Halide with Broad Light Emission and Selective H_2O Vapor Sorption. *Angew. Chem., Int. Ed.* **2023**, *62*, No. e202218429.

(20) Ray, A. B. Activated carbon. *Ind. Eng. Chem.* **1940**, *32*, 1166−1167.

(21) Davis, M. E.; Lobo, R. F. Zeolite and molecular sieve synthesis. *Chem. Mater.* **1992**, *4*, 756−768.

(22) Behrman, A. S. Recent developments in zeolite softening. *Ind. Eng. Chem.* **1927**, *19*, 445−447.

(23) Vermeiren, W.; Gilson, J. P. Impact of Zeolites on the Petroleum and Petrochemical Industry. *Top. Catal.* **2009**, *52*, 1131−1161.

(24) Rimer, J. D.; Kumar, M.; Li, R.; Lupulescu, A. I.; Oleksiak, M. D. Tailoring the physicochemical properties of zeolite catalysts. *Catal. Sci. Technol.* **2014**, *4*, 3762−3771.

(25) Phan, A.; Doonan, C. J.; Uribe-Romo, F. J.; Knobler, C. B.; O'Keeffe, M.; Yaghi, O. M. Synthesis, Structure, and Carbon Dioxide Capture Properties of Zeolitic Imidazolate Frameworks. *Acc. Chem. Res.* **2010**, *43*, 58−67.

(26) Kondo, M.; Yoshitomi, T.; Matsuzaka, H.; Kitagawa, S.; Seki, K. Three-Dimensional Framework with Channeling Cavities for Small Molecules: $\{[M_2(4,4'\text{-bpy})_3(NO_3)_4]\cdot xH_2O\}n$ (M:Co, Ni, Zn). *Angew. Chem., Int. Ed. Engl.* **1997**, *36*, 1725−1727.

(27) Hanikel, N.; Pei, X.; Chheda, S.; Lyu, H.; Jeong, W.; Sauer, J.; Gagliardi, L.; Yaghi, O. M. Evolution of water structures in metal-organic frameworks for improved atmospheric water harvesting. *Science* **2021**, *374*, 454−459.

(28) Alezi, D.; Oppenheim, J. J.; Sarver, P. J.; Iliescu, A.; Dinakar, B.; Dinca, M. Tunable Low-Relative Humidity and High-Capacity Water Adsorption in a Bibenzotriazole Metal-Organic Framework. *J. Am. Chem. Soc.* **2023**, *145*, 25233−25241.

(29) Hajra, S.; Sahu, M.; Padhan, A. M.; Lee, I. S.; Yi, D. K.; Alagarsamy, P.; Nanda, S. S.; Kim, H. J. A Green Metal-Organic Framework-Cyclodextrin MOF: A Novel Multifunctional Material Based Triboelectric Nanogenerator for Highly Efficient Mechanical Energy Harvesting. *Adv. Funct. Mater.* **2021**, *31*, 2101829.

(30) Uhlir, A., Jr Electrolytic Shaping of Germanium and Silicon. *Bell Syst. Tech. J.* **1956**, *35*, 333−347.

(31) Beale, M. I. J.; Benjamin, J. D.; Uren, M. J.; Chew, N. G.; Cullis, A. G. An experimental and theoretical study of the formation and microstructure of porous silicon. *J. Cryst. Growth* **1985**, *73*, 622−636.

(32) Monaico, E.; Tiginyanu, I.; Ursaki, V. Porous semiconductor compounds. *Semicond. Sci. Technol.* **2020**, *35*, 103001.

(33) Föll, H.; Carstensen, J.; Frey, S. Porous and Nanoporous Semiconductors and Emerging Applications. *J. Nanomater.* **2006**, *2006*, 091635.
(34) Cullis, A. G.; Canham, L. T.; Calcott, P. D. J. The structural and luminescence properties of porous silicon. *J. Appl. Phys.* **1997**, *82*, 909−965.
(35) Parkhutik, V. Porous silicon—mechanisms of growth and applications. *Solid-State Electron.* **1999**, *43*, 1121−1141.
(36) Isaiev, M.; Tutashkonko, S.; Jean, V.; Termentzidis, K.; Nychyporuk, T.; Andrusenko, D.; Marty, O.; Burbelo, R. M.; Lacroix, D.; Lysenko, V. Thermal conductivity of meso-porous germanium. *Appl. Phys. Lett.* **2014**, *105*, 031912.
(37) Armatas, G. S.; Kanatzidis, M. G. Hexagonal Mesoporous Germanium. *Science* **2006**, *313*, 817−820.
(38) Erné, B. H.; Vanmaekelbergh, D.; Kelly, J. J. Morphology and Strongly Enhanced Photoresponse of GaP Electrodes Made Porous by Anodic Etching. *J. Electrochem. Soc.* **1996**, *143*, 305.
(39) Reid, M.; Cravetchi, I.; Fedosejevs, R.; Tiginyanu, I. M.; Sirbu, L.; Boyd, R. W. Enhanced nonlinear optical response of InP(100) membranes. *Phys. Rev. B* **2005**, *71*, 081306.
(40) Alshehri, B.; Lee, S.-M.; Kang, J.-H.; Gong, S.-H.; Ryu, S.-W.; Cho, Y.-H.; Dogheche, E. Optical waveguiding properties into porous gallium nitride structures investigated by prism coupling technique. *Appl. Phys. Lett.* **2014**, *105*, 051906.
(41) Tenne, R.; Hodes, G. Improved efficiency of CdSe photoanodes by photoelectrochemical etching. *Appl. Phys. Lett.* **1980**, *37*, 428−430.
(42) Filip, M. R.; Eperon, G. E.; Snaith, H. J.; Giustino, F. Steric engineering of metal-halide perovskites with tunable optical band gaps. *Nat. Commun.* **2014**, *5*, 5757.
(43) Kim, G. Y.; Senocrate, A.; Yang, T.-Y.; Gregori, G.; Grätzel, M.; Maier, J. Large tunable photoeffect on ion conduction in halide perovskites and implications for photodecomposition. *Nat. Mater.* **2018**, *17*, 445−449.
(44) Manser, J. S.; Christians, J. A.; Kamat, P. V. Intriguing Optoelectronic Properties of Metal Halide Perovskites. *Chem. Rev.* **2016**, *116*, 12956−13008.
(45) Tu, Q.; Spanopoulos, I.; Yasaei, P.; Stoumpos, C. C.; Kanatzidis, M. G.; Shekhawat, G. S.; Dravid, V. P. Stretching and Breaking of Ultrathin 2D Hybrid Organic-Inorganic Perovskites. *ACS Nano* **2018**, *12*, 10347−10354.
(46) Angmo, D.; Yan, S.; Liang, D.; Scully, A. D.; Chesman, A. S. R.; Kellam, M.; Duffy, N. W.; Carter, N.; Chantler, R.; Chen, C.; Gao, M. Toward Rollable Printed Perovskite Solar Cells for Deployment in Low-Earth Orbit Space Applications. *ACS Appl. Energy Mater.* **2024**, *7*, 1777−1791.
(47) Wang, P.; Wu, Y.; Cai, B.; Ma, Q.; Zheng, X.; Zhang, W.-H. Solution-Processable Perovskite Solar Cells toward Commercialization: Progress and Challenges. *Adv. Funct. Mater.* **2019**, *29*, 1807661.
(48) Zhao, D.; Yu, Y.; Wang, C.; Liao, W.; Shrestha, N.; Grice, C. R.; Cimaroli, A. J.; Guan, L.; Ellingson, R. J.; Zhu, K.; Zhao, X.; Xiong, R.-G.; Yan, Y. Low-bandgap mixed tin-lead iodide perovskite absorbers with long carrier lifetimes for all-perovskite tandem solar cells. *Nat. Energy* **2017**, *2*, 17018.
(49) Stranks, S. D.; Eperon, G. E.; Grancini, G.; Menelaou, C.; Alcocer, M. J. P.; Leijtens, T.; Herz, L. M.; Petrozza, A.; Snaith, H. J. Electron-Hole Diffusion Lengths Exceeding 1 Micrometer in an Organometal Trihalide Perovskite Absorber. *Science* **2013**, *342*, 341−344.
(50) Dong, Q.; Fang, Y.; Shao, Y.; Mulligan, P.; Qiu, J.; Cao, L.; Huang, J. Electron-hole diffusion lengths > 175 μm in solution-grown $CH_3NH_3PbI_3$ single crystals. *Science* **2015**, *347*, 967−970.
(51) Wei, H.; Huang, J. Halide lead perovskites for ionizing radiation detection. *Nat. Commun.* **2019**, *10*, 1066.
(52) Kanaya, S.; Kim, G. M.; Ikegami, M.; Miyasaka, T.; Suzuki, K.; Miyazawa, Y.; Toyota, H.; Osonoe, K.; Yamamoto, T.; Hirose, K. Proton Irradiation Tolerance of High-Efficiency Perovskite Absorbers for Space Applications. *J. Phys. Chem. Lett.* **2019**, *10*, 6990−6995.
(53) Reb, L. K.; Böhmer, M.; Predeschly, B.; Grott, S.; Weindl, C. L.; Ivandekic, G. I.; Guo, R.; Dreißigacker, C.; Gernhäuser, R.; Meyer, A.; Müller-Buschbaum, P. Perovskite and Organic Solar Cells on a Rocket Flight. *Joule* **2020**, *4*, 1880−1892.
(54) Yin, W.-J.; Shi, T.; Yan, Y. Unique Properties of Halide Perovskites as Possible Origins of the Superior Solar Cell Performance. *Adv. Mater.* **2014**, *26*, 4653−4658.
(55) Lang, F.; Nickel, N. H.; Bundesmann, J.; Seidel, S.; Denker, A.; Albrecht, S.; Brus, V. V.; Rappich, J.; Rech, B.; Landi, G.; Neitzert, H. C. Radiation Hardness and Self-Healing of Perovskite Solar Cells. *Adv. Mater.* **2016**, *28*, 8726−8731.
(56) Yu, W.; Batchelor-McAuley, C.; Chang, X.; Young, N. P.; Compton, R. G. Porosity controls the catalytic activity of platinum nanoparticles. *Phys. Chem. Chem. Phys.* **2019**, *21*, 20415−20421.
(57) Chen, H.; Liang, X.; Liu, Y.; Ai, X.; Asefa, T.; Zou, X. Active Site Engineering in Porous Electrocatalysts. *Adv. Mater.* **2020**, *32*, 2002435.
(58) Li, P.-Z.; Wang, X.-J.; Liu, J.; Lim, J. S.; Zou, R.; Zhao, Y. A Triazole-Containing Metal-Organic Framework as a Highly Effective and Substrate Size-Dependent Catalyst for CO_2 Conversion. *J. Am. Chem. Soc.* **2016**, *138*, 2142−2145.
(59) Kerner, R. A.; Rand, B. P. Ionic-Electronic Ambipolar Transport in Metal Halide Perovskites: Can Electronic Conductivity Limit Ionic Diffusion? *J. Phys. Chem. Lett.* **2018**, *9*, 132−137.
(60) Tress, W. Metal Halide Perovskites as Mixed Electronic-Ionic Conductors: Challenges and Opportunities—From Hysteresis to Memristivity. *J. Phys. Chem. Lett.* **2017**, *8*, 3106−3114.
(61) Lu, X.; Zhao, X.; Ding, S.; Hu, X. 3D mixed ion/electron-conducting scaffolds for stable sodium metal anodes. *Nanoscale* **2024**, *16*, 3379−3392.
(62) Cao, D.; Zhang, Y.; Ji, T.; Zhao, X.; Cakmak, E.; Ozcan, S.; Geiwitz, M.; Bilheux, J.; Xu, K.; Wang, Y.; Burch, K. S.; Tu, Q. H.; Zhu, H. Li Dynamics in Mixed Ionic-Electronic Conducting Interlayer of All-Solid-State Li-metal Batteries. *Nano Lett.* **2024**, *24*, 1544−1552.
(63) Armatas, G. S.; Kanatzidis, M. G. Mesostructured germanium with cubic pore symmetry. *Nature* **2006**, *441*, 1122−1125.
(64) Quill, N.; Green, L.; O'Dwyer, C.; Buckley, D. N.; Lynch, R. P. Electrochemical Pore Formation in InP: Understanding and Controlling Pore Morphology. *ECS Trans.* **2017**, *75*, 29.
(65) Petkovich, N. D.; Stein, A. Controlling macro- and mesostructures with hierarchical porosity through combined hard and soft templating. *Chem. Soc. Rev.* **2013**, *42*, 3721−3739.
(66) Ryoo, R.; Joo, S. H.; Jun, S. Synthesis of Highly Ordered Carbon Molecular Sieves via Template-Mediated Structural Transformation. *J. Phys. Chem. B* **1999**, *103*, 7743−7746.
(67) Li, X.-X.; Zheng, S.-T. Three-dimensional metal-halide open frameworks. *Coord. Chem. Rev.* **2021**, *430*, 213663.
(68) Li, X.; Do, T. T. H.; Granados del Águila, A.; Huang, Y.; Chen, W.; Xiong, Q.; Zhang, Q. A 3D Haloplumbate Framework Constructed From Unprecedented Lindqvist-like Highly Coordinated $[Pb_6Br_{25}]_{13}$- Nanoclusters with Temperature-Dependent Emission. *Chem. Asian J.* **2018**, *13*, 3185−3189.
(69) Yue, C.-Y.; Yue, Y.-D.; Sun, H.-X.; Li, D.-Y.; Lin, N.; Wang, X.-M.; Jin, Y.-X.; Dong, Y.-H.; Jing, Z.-H.; Lei, X.-W. Transition metal complex dye-sensitized 3D iodoplumbates: syntheses, structures and photoelectric properties. *Chem. Commun.* **2019**, *55*, 6874−6877.
(70) Hao, P.; Zhang, L.; Shen, J.; Fu, Y. Structural and photochromic modulation of dimethylbenzotriazolium iodoargentate hybrid materials. *Dyes Pigm.* **2018**, *153*, 284−290.
(71) Wang, G.-E.; Xu, G.; Wang, M.-S.; Cai, L.-Z.; Li, W.-H.; Guo, G.-C. Semiconductive 3-D haloplumbate framework hybrids with high color rendering index white-light emission. *Chem. Sci.* **2015**, *6*, 7222−7226.
(72) Sun, A.-H.; Han, S.-D.; Pan, J.; Li, J.-H.; Wang, G.-M.; Wang, Z.-H. 3D Inorganic Cuprous Iodide Open-Framework Templated by In Situ N-Methylated 2,4,6-Tri(4-pyridyl)-1,3,5-triazine. *Cryst. Growth Des.* **2017**, *17*, 3588−3591.
(73) Kataoka, S.; Banerjee, S.; Kawai, A.; Kamimura, Y.; Choi, J.-C.; Kodaira, T.; Sato, K.; Endo, A. Layered Hybrid Perovskites with

https://doi.org/10.1021/acsorginorgau.4c00093
ACS Org. Inorg. Au 2025, 5, 87−96

Micropores Created by Alkylammonium Functional Silsesquioxane Interlayers. *J. Am. Chem. Soc.* **2015**, *137*, 4158−4163.
(74) Kataoka, S.; Kamimura, Y.; Endo, A. Toward Increasing Micropore Volume between Hybrid Layered Perovskites with Silsesquioxane Interlayers. *Langmuir* **2018**, *34*, 4166−4172.
(75) Wang, W.; Yang, H.; Chen, Y.; Bu, X.; Feng, P. Cyclobutanedicarboxylate Metal-Organic Frameworks as a Platform for Dramatic Amplification of Pore Partition Effect. *J. Am. Chem. Soc.* **2023**, *145*, 17551−17556.
(76) Gómez-Gualdrón, D. A.; Moghadam, P. Z.; Hupp, J. T.; Farha, O. K.; Snurr, R. Q. Application of Consistency Criteria To Calculate BET Areas of Micro- And Mesoporous Metal-Organic Frameworks. *J. Am. Chem. Soc.* **2016**, *138*, 215−224.
(77) Cai, S.-L.; Zhang, Y.-B.; Pun, A. B.; He, B.; Yang, J.; Toma, F. M.; Sharp, I. D.; Yaghi, O. M.; Fan, J.; Zheng, S.-R.; Zhang, W.-G.; Liu, Y. Tunable electrical conductivity in oriented thin films of tetrathiafulvalene-based covalent organic framework. *Chem. Sci.* **2014**, *5*, 4693−4700.
(78) Li, J.; Zhou, K.; Liu, J.; Zhen, Y.; Liu, L.; Zhang, J.; Dong, H.; Zhang, X.; Jiang, L.; Hu, W. Aromatic Extension at 2,6-Positions of Anthracene toward an Elegant Strategy for Organic Semiconductors with Efficient Charge Transport and Strong Solid State Emission. *J. Am. Chem. Soc.* **2017**, *139*, 17261−17264.
(79) Liu, Y.; Wei, Y.; Liu, M.; Bai, Y.; Wang, X.; Shang, S.; Du, C.; Gao, W.; Chen, J.; Liu, Y. Face-to-Face Growth of Wafer-Scale 2D Semiconducting MOF Films on Dielectric Substrates. *Adv. Mater.* **2021**, *33*, 2007741.
(80) Byun, Y.; Xie, L. S.; Fritz, P.; Ashirov, T.; Dinca, M.; Coskun, A. A Three-Dimensional Porous Organic Semiconductor Based on Fully sp2-Hybridized Graphitic Polymer. *Angew. Chem., Int. Ed.* **2020**, *59*, 15166−15170.
(81) Bi, S.; Yang, C.; Zhang, W.; Xu, J.; Liu, L.; Wu, D.; Wang, X.; Han, Y.; Liang, Q.; Zhang, F. Two-dimensional semiconducting covalent organic frameworks via condensation at arylmethyl carbon atoms. *Nat. Commun.* **2019**, *10*, 2467.
(82) Zhou, X.; Cheng, X.; Zhu, Y.; Elzatahry, A. A.; Alghamdi, A.; Deng, Y.; Zhao, D. Ordered porous metal oxide semiconductors for gas sensing. *Chin. Chem. Lett.* **2018**, *29*, 405−416.
(83) Saparov, B.; Mitzi, D. B. Organic-Inorganic Perovskites: Structural Versatility for Functional Materials Design. *Chem. Rev.* **2016**, *116*, 4558−4596.
(84) An, J.; Rosi, N. L. Tuning MOF CO_2 Adsorption Properties via Cation Exchange. *J. Am. Chem. Soc.* **2010**, *132*, 5578−5579.
(85) Li, X.; Ha Do, T. T.; Granados del Águila, A.; Huang, Y.; Chen, W.; Li, Y.; Ganguly, R.; Morris, S.; Xiong, Q.; Li, D.-s.; Zhang, Q. Two-Dimensional and Emission-Tunable: An Unusual Perovskite Constructed from Lindqvist-Type $[Pb_6Br_{19}]^{7-}$ Nanoclusters. *Inorg. Chem.* **2018**, *57*, 14035−14038.
(86) Chakraborty, S.; Petel, B. E.; Schreiber, E.; Matson, E. M. Atomically precise vanadium-oxide clusters. *Nanoscale Adv.* **2021**, *3*, 1293−1318.
(87) Azmy, A.; Zhao, X.; Angeli, G. K.; Welton, C.; Raval, P.; Wojtas, L.; Zibouche, N.; Manjunatha Reddy, G. N.; Trikalitis, P. N.; Cai, J.; Spanopoulos, I. One-Year Water-Stable and Porous Bi(III) Halide Semiconductor with Broad-Spectrum Antibacterial Performance. *ACS Appl. Mater. Interfaces* **2023**, *15*, 42717−42729.
(88) Xiao, C.; Tian, J.; Chen, Q.; Hong, M. Water-stable metal-organic frameworks (MOFs): rational construction and carbon dioxide capture. *Chem. Sci.* **2024**, *15*, 1570−1610.
(89) Ockwig, N. W.; Nenoff, T. M. Membranes for Hydrogen Separation. *Chem. Rev.* **2007**, *107*, 4078−4110.
(90) McDonagh, A. W.; McNeil, B. L.; Patrick, B. O.; Ramogida, C. F. Synthesis and Evaluation of Bifunctional [2.2.2]-Cryptands for Nuclear Medicine Applications. *Inorg. Chem.* **2021**, *60*, 10030−10037.
(91) Lehn, J. M. Cryptates: macropolycyclic inclusion complexes. *Pure Appl. Chem.* **1977**, *49*, 857−870.
(92) Ben Ali, S.; Feki, A.; Ferretti, V.; Nasri, M.; Belhouchet, M. Crystal Structure, Spectroscopic Measurement, Optical Properties, Thermal Studies and Biological Activities of a New Hybrid Material Containing Iodide Anions of Bismuth(iii). *RSC Adv.* **2020**, *10*, 35174−35184.
(93) Turk, K.; Grzeskiewicz, A. M.; Banti, C. N.; Hadjikakou, S. K.; Kubicki, M.; Ozturk, I. I. Synthesis, Characterization, and Biological Properties of mono-, di- and Poly-nuclear Bismuth(III) Halide Complexes Containing Thiophene-2-carbaldehyde Thiosemicarbazones. *J. Inorg. Biochem.* **2022**, *237*, 111987.
(94) Zhang, X.; Zhang, G.; Chai, M.; Yao, X.; Chen, W.; Chu, P. K. Synergistic antibacterial activity of physical-chemical multi-mechanism by TiO_2 nanorod arrays for safe biofilm eradication on implant. *Bioact. Mater.* **2021**, *6*, 12−25.
(95) Liang, X.; Dai, R.; Ma, H.; Tang, X.; Zhang, B. Synergistic antibacterial properties of ZnO-SnO_2 composite under both light and dark conditions. *Ceram. Int.* **2022**, *48*, 32089−32103.
(96) Sun, S.; Liu, M.; Thapa, J.; Hartono, N. T. P.; Zhao, Y.; He, D.; Wieghold, S.; Chua, M.; Wu, Y.; Bulović, V.; Ling, S.; Brabec, C. J.; Cooper, A. I.; Buonassisi, T. Cage Molecules Stabilize Lead Halide Perovskite Thin Films. *Chem. Mater.* **2022**, *34*, 9384−9391.

https://doi.org/10.1021/acsorginorgau.4c00093
ACS Org. Inorg. Au 2025, 5, 87−96